



# Triclosan-induced neuroinflammation develops caspase-independent and TNF- $\alpha$ signaling pathway associated necroptosis in Neuro-2a cells



Parul Katiyar<sup>1</sup>, Somesh Banerjee, Sandip Nathani, Partha Roy<sup>\*,2</sup>

Molecular Endocrinology Laboratory, Department of Biosciences and Bioengineering, Indian Institute of Technology Roorkee, Roorkee 247667, Uttarakhand, India

## ARTICLE INFO

**Keywords:**  
Triclosan  
Neuro-2a  
Autophagy  
Necroptosis  
Tau pathogenesis

## ABSTRACT

Triclosan (TCS) is widely used in cosmetics and healthcare industry as a broad-spectrum antibacterial agent. The lipophilic property and persistent nature of TCS has led to severe health issues. In the present study, we have evaluated the neuroinflammatory effect of TCS on mouse Neuro-2a cells. Initial investigation confirmed a dose-dependent loss in viability and morphology of cells in presence of TCS. The transcription and translation studies confirmed a downregulation in the expression of autophagy markers in Neuro-2a cells. The confocal microscopy study revealed that the abrogated autophagy in TCS-treated cells occurred due to loss in the autophagy flux and prevention in the lipidation of autophagosome bilayer. The fluorescence microscopy also confirmed a loss in the formation of autophagolysosomes in neuronal cells with increasing TCS concentrations. TCS treatment resulted in loss of mitochondrial integrity in cells as evidenced by a decrease in mitochondrial membrane potential in JC-1 staining. Further, the transcriptional and translational studies confirmed the activation of TNF- $\alpha$  signaling pathway in TCS-treated cells thus enhancing the expression of RIPK1, RIPK3 and MLKL proteins and their phosphorylated forms. TCS was also found to increase the tau protein pathogenesis in Neuro-2a cells, which alludes to the development of tau-associated neurodegeneration. Altogether, this study confirms the neuroinflammatory actions of TCS in Neuro-2a cells involving a TNF- $\alpha$ -induced MLKL-mediated signaling.

## 1. Introduction

Triclosan (2,4,4'-trichloro-2'-hydroxydiphenyl ether, TCS) is a synthetic, lipid-soluble antimicrobial agent that was first employed in the healthcare industry in surgical scrubs and in handwashing before surgery to prevent microbial infections. The broad-spectrum antibacterial property of TCS led to its introduction in personal care products (e.g., hand soaps, toothpaste, detergents, cosmetics, hair cleansers, body spray, shave gel), household products (e.g., kitchenware, wet mop heads, cutting boards, clothing) (Bedoux et al., 2012; Liao and Kannan, 2014). The utilization of TCS has raised concerns over time. The Florence Statement on Triclosan and Triclocarban documents the health problems associated with the usage of TCS in personal care products (Halden et al., 2017). TCS has also been reported extensively as a potential endocrine-disrupting chemical in multiple species (Raut and Angus, 2010; Wang et al., 2015). The chemical properties of TCS, mainly lipophilicity and the ability to cross biological barriers including blood-brain barrier, lead to its bioaccumulation (Dhillon et al.,

2015; Geens et al., 2012). TCS and its transformed products, such as methyl triclosan and dioxins, generate toxic effects, especially on animals.

In recent times, several studies were performed to evaluate the effect of TCS on generation of disease conditions (Muth-Köhne et al., 2012). TCS was found to be reportedly present in the hypothalamus region and white matter of brain in a recent cohort study (Van Der Meer et al., 2017). It has been earlier reported that TCS delays the development of secondary motor neurons in zebrafish (Muth-Köhne et al., 2012). It was also found to generate apoptotic bodies by inducing the extrinsic apoptosis in primary neocortical neuron culture by inducing Fas receptor-mediated caspase-3 (CASP3) activation (Szychowski et al., 2015) and altered the reactive oxygen species (ROS) homeostasis in neural stem cells. In an earlier study, TCS was reported to compromise the anti-oxidant defense system of neurons by reducing the glutathione activity (Park et al., 2016). TCS also enhances the estrogen receptor-mediated signaling, supporting the progression of breast and ovarian cancer in human population

\* Corresponding author.

E-mail addresses: [pkatiyar@bt.iitr.ac.in](mailto:pkatiyar@bt.iitr.ac.in) (P. Katiyar), [sbanerjee1@bt.iitr.ac.in](mailto:sbanerjee1@bt.iitr.ac.in) (S. Banerjee), [snathani@bt.iitr.ac.in](mailto:snathani@bt.iitr.ac.in) (S. Nathani), [partha.roy@bt.iitr.ac.in](mailto:partha.roy@bt.iitr.ac.in) (P. Roy).

<sup>1</sup> ORCID ID: 0000-0002-0678-0285.

<sup>2</sup> ORCID ID: 0000-0003-1943-3079.

(Kim et al., 2014; Lee et al., 2014). The functioning of hepatocytes was also observed to be affected in the presence of TCS due to augmentation of catabolism process and disturbing the thyroid hormone homeostasis (Paul et al., 2010). TCS was also reported to enhance the level of pro-inflammatory cytokines like IL-1 $\beta$ , IL-6, TNF- $\alpha$  and IFN- $\gamma$ , in human immune cells (Wilburn et al., 2021). In a recent study TCS was found to cause neurotoxicity in mice brain thus disrupting locomotor activity and motor coordination (Tabari et al., 2019). TCS also has a negative impact on hippocampal-based spatial memory performance (Arias-cavieres et al., 2018). All these studies substantiated the existing reports on the harmful effect of environmental toxicants like TCS.

Several earlier studies have reported that excessive ROS production leads to generation of inflammatory responses in cells. Since TCS has been a potent protonophoric agent, it was intriguing to check a relation between TCS and neuroinflammation. To clarify this cross-talk, in the present study, we attempted to investigate the neuroinflammatory potential of TCS in Neuro-2a cells and ultimately analyzing its impacts on tauopathy or tau-mediated pathogenesis.

## 2. Materials & methods

### 2.1. Cell culture

The mouse neuroblastoma Neuro-2a cell line was procured from National Centre for Cell Sciences (NCCS), Pune, India. The cells were maintained as a monolayer using Dulbecco's Modified Essential Media (DMEM) (Cat. No. AT-007, Himedia, Mumbai, India) supplemented with 10% FBS (Cat. No. 11573397) and 1% antibiotic-antimycotic solution (Cat. No. 15240062, both from Gibco, Thermo Fisher Scientific, Waltham, MA, USA) at 37 °C in a humidified incubator with 95% air along with 5% CO<sub>2</sub> (MCO-15AC, SANYO Electric Co., Ltd. JAPAN).

### 2.2. Cell viability assay

The viability of Neuro-2a cells in the presence of a different concentration of TCS (1, 10, 30 and 50  $\mu$ M) (Cat. No. T1872, Tokyo Chemical Industry Co., Ltd., Tokyo, Japan; Purity > 98.0%) was determined by performing MTT [3-(4,5-dimethylthiazol-2-yl)-2,5-diphenyl tetrazolium bromide] assay (Mosmann, 1983). Briefly, 5,000 cells in 200  $\mu$ l media were seeded in each well of the 96-wells plate to form the adherent monolayer. After 24 h, media from each well was replaced with fresh media supplemented with varying TCS concentrations. TCS was dissolved in DMSO (Cat. No. TC185, Himedia, Mumbai, India) and added 0.1% v/v with media in respective wells in the entire study. Further, the cells treated with only DMSO (0.1% v/v) were considered as control groups in all the experiments. After 24 h, the media was supplemented with 20  $\mu$ l of MTT dye (Cat. No. TC191, Himedia, Mumbai, India) (5 mg/ml in Phosphate Buffered Saline, PBS), and the cells were incubated for another 4 h at 37 °C. Then the media from each well was aspirated, and formed formazan crystals were dissolved in 200  $\mu$ l DMSO. The absorbance was measured at 570 nm using FLOUstar optima (BMG labtech, Germany) microplate-reader. The cell viability percentage was calculated by using the formula:

(Mean absorbance of TCS treated cells/Mean absorbance of DMSO treated cells)  $\times$  100.

It is to be noted that the dosage of TCS and duration of its exposure to the cells were based on some earlier reports (Park et al., 2016; Wang et al., 2019). Further, our preliminary experiments showed that the treatment of cells with TCS with our selected dosages for 24 h caused a remarkable physiological effect on cells which at 48 h seemed to be more of toxic in nature (data not shown). This was another reason of choosing the said time period for all subsequent experiments. Also, the dosage of TCS used in this study was within the range that has

been reported to be present in biological fluids and confirming same or similar exposure conditions (Liu et al., 2021).

### 2.3. DNA fragmentation assay

The analysis of the appearance of genomic DNA cleavage pattern was performed by agarose gel electrophoresis according to the method mentioned previously (Varshney et al., 2017). Briefly, Neuro-2a cells were treated with varying concentrations of TCS for 24 h. Thereafter, the cells were first harvested and then washed with PBS followed by suspension of resultant pellet in 500  $\mu$ l of lysis buffer (10 mM Tris HCl pH 8.0, 10 mM EDTA and 0.5% Triton X-100). The resulting solution was then treated to remove RNA content using 0.1 mg/ml concentration of DNase-free RNase for 60 min at 37 °C. After this, an equal volume of phenol, chloroform, and isoamyl alcohol mixture in the respective ratio of 25:24:1 was added. Then the mixture was centrifuged at 20,814  $\times$  g for 3 min at room temperature. The obtained supernatant was again mixed with an equal volume of chloroform and further centrifuged three times. Then the genomic DNA was precipitated by adding an equal volume of ethanol supplemented with 0.3 mM sodium acetate to the supernatant obtained in the previous step. The resultant pellet was washed with 70% ethanol twice and suspended in 20  $\mu$ l of nuclease-free water. Finally, the extracted DNA was separated on 2% agarose gel containing 0.4  $\mu$ g/ml ethidium bromide electrophoretically and photographed under the gel documentation system (Bio-Rad Laboratories, Inc., Hercules, CA, USA).

### 2.4. Acridine orange/ethidium bromide dual staining

In order to visualize the nuclear changes and formation of characteristic apoptotic bodies inside cells, they were stained with Acridine orange (AO)/Ethidium bromide (EB) dye mixture as described previously (Kasibhatla, 2006). Briefly,  $5 \times 10^5$  cells were seeded in a six-well plate and treated with 1, 10, 30, and 50  $\mu$ M concentrations of TCS for 24 h. The cells were then washed gently in PBS followed by treatment with 500  $\mu$ l of AO/EB dye mixture (both 100  $\mu$ g/ml in PBS) (Cat. No. 318337 and E28751, Sigma, St. Louis, MO, USA) to each well, and the cells were visualized under a fluorescent microscope (EVOS® FL Cell Imaging System, Thermo Fisher Scientific, Waltham, MA, USA).

### 2.5. Monodansylcadaverine (MDC) staining for determining autophagy vacuoles formation

MDC is a fluorescent compound used to trace autophagic vacuoles in cells (Boland et al., 2008). Neuro-2a cells were treated for 24 h with various concentrations of TCS and temsirolimus (0.2  $\mu$ M) (Cat. No. PZ0020 Sigma, St. Louis, MO, USA) used as positive control. Temsirolimus is an ester analog of rapamycin. It binds and inhibits the mammalian target of rapamycin (mTOR), resulting in an increased autophagic process in any cell. The cells were then stained with 0.5 mM MDC (Cat. No. D4008, Sigma, St. Louis, MO, USA) (dissolved in PBS) for another 30 min at 37 °C. Thereafter, the cells were gently washed with PBS twice and fixed with 4% formaldehyde and further analyzed under a fluorescent microscope (Thermo Fisher Scientific, Waltham, MA, USA) at 355 and 460 excitations and emission, respectively. AO was used to counter-stain the cells.

### 2.6. LC3-puncta assay

The LC3-puncta assay was performed to monitor the autophagy vesicle formation in Neuro-2a cells in response to TCS treatment according to a method described earlier (Jackson et al., 2005). For this assay, Neuro-2a cells were transiently transfected with 2  $\mu$ g of EGFP-LC3 plasmid [containing mammalian LC3 coding gene insert downstream of EGFP, (plasmid # 11546) procured from ADDgene plasmid

reservoir, Cambridge, MA, USA], using Ultra<sup>293</sup> transfection reagent as per the manufacturer's protocol (Cat. No. MB056, GeneDireX Inc., Taoyuan, Taiwan). After 24 h of transfection, the cells were treated with different concentrations of TCS (10, 30 and 50  $\mu\text{M}$ ) and temsirolimus (0.2  $\mu\text{M}$ , as positive control) for another 24 h. On completion of the incubation, the cells were then fixed with 4% formaldehyde, followed by gentle PBS washing and observed under a confocal laser scanning microscope (LSM 780, Carl Zeiss, Germany) for puncta formation.

### 2.7. Lysosome labeling with lysotracker staining

Lysotracker Red DND99 is used for labeling active lysosomes in cells. Neuro-2a cells were seeded in a 6-well plate for 24 h and then treated with various concentrations of TCS (10, 30 and 50  $\mu\text{M}$ ) and temsirolimus (0.2  $\mu\text{M}$ ) for 24 h. After incubation, the cells were treated with DND99 red (Cat. No. L7528, Thermo Fisher Scientific, Waltham, MA, USA) for another half hour at 37 °C. The cells were then fixed with 4% formaldehyde for 15 min at room temperature in the dark followed by washing with PBS two times and staining with AO at room temperature. Then the slides were prepared and observed under confocal laser scanning microscopy (LSM 780, Carl Zeiss, Germany).

### 2.8. Mitochondrial probing for the measurement of membrane potential

The impact of TCS on mitochondrial membrane potential ( $\Delta\psi\text{m}$ ) of Neuro-2a cells was examined using JC-1 fluorescent probe (Cat. No. KTA4001, Abbkine Scientific Co., Ltd., Wuhan, China). The Neuro-2a cells were seeded in a 6-well plate for 24 h and then treated with various concentration of TCS (10, 30 and 50  $\mu\text{M}$ ) for 24 h along with control condition. The cells treated with 20  $\mu\text{M}$  carbonyl cyanide 3-chlorophenylhydrazone (CCCP) for 30 min was considered as positive control. After respective incubation time period, the cells were stained with JC-1 staining solution (100  $\mu\text{l/ml}$  media) for 30 min and observed under fluorescent microscope (EVOS® FL Cell Imaging System, Thermo Fisher Scientific, Waltham, MA, USA).

### 2.9. RNA isolation and reverse transcription polymerase chain reaction

After treating Neuro-2a cells with different concentrations of TCS, the total RNA was isolated using RNA X-Press reagent (Cat. No. MB601, Himedia, Mumbai, India) as per manufacturer's instructions and quantified. Then 2  $\mu\text{g}$  of RNA from each sample was reverse transcribed to cDNA using RevertAid First Strand cDNA synthesis kit (Cat. No. K1621, Thermo Fisher Scientific, Waltham, MA, USA). The gene expression analysis was performed by quantitative PCR (RT-qPCR) using primers, as mentioned in Table 1. The study was performed using SYBR green master mix (Cat. No. A25742; PowerUp™ SYBR™ Green Master Mix, Applied Biosystems, Thermo Fischer Scientific, Waltham, MA, USA,) using RT-qPCR equipment (Applied Biosystems™ QuantStudio™ 5, Thermo Fischer Scientific, Waltham, MA, USA). A comparative  $2^{-\Delta\Delta C_T}$  method was employed to determine the relative mRNA expression of test genes (Livak and Schmittgen, 2001).  $\beta$ -Actin was used as an internal control for our entire PCR analysis, which was carried out three independent times.

### 2.10. Immunoblot analysis

The total protein of Neuro-2a cells treated at different conditions as mentioned previously, was isolated using RIPA lysis buffer (Cat. No. TC131, Himedia, Mumbai, India) supplemented with 1X protease inhibitor cocktail (Cat. No. ML051, Himedia, Mumbai, India). The isolated protein was quantified using the BCA protein quantification kit (Cat. No. 71258-M, Sigma, St. Louis, MO, USA). Then 40  $\mu\text{g}$  of each sample was electrophoretically separated on 8–12% polyacrylamide gel and electro-transferred on to PVDF membrane. The membranes were then

blocked using 3% BSA in TBS-T buffer for 2 h. Then the membranes were incubated overnight at 4 °C in TBS-T buffer supplemented with primary antibodies the details of which are mentioned in Table 2. Then the blots were washed with TBS-T buffer for 10 min thrice and again incubated for around 2 h in secondary antibody (1:10,000). The blots were then developed in dark conditions using the ECL kit (Bio-Rad Laboratories, Inc., Hercules, California, USA), and the developed blots were photographed, and densitometric analysis was performed using ImageJ software (NIH, Bethesda, MD, USA) using  $\beta$ -Actin as an internal control.

### 2.11. Statistical analysis

All data is represented as Mean  $\pm$  SEM of three independently performed experiments. Statistical evaluation was performed by one-way ANOVA followed by Tukey's post hoc test using Graph Pad Prism 6 software (Graph Pad Software, San Diego, CA, USA). The data analysis was considered statistically significant at  $p$  value  $<$  0.05.

## 3. Results

### 3.1. Effect of TCS on viability and morphology of Neuro-2a cells

The effect of TCS on the viability of Neuro-2a cells was determined by performing colorimetric MTT assay. The results confirmed that the cells retained the viability at 1, 10 and 30  $\mu\text{M}$  concentrations of TCS (Fig. 1a). At higher concentration of TCS (50  $\mu\text{M}$ ), a minor but significant decline in the cell viability was observed. (Fig. 1a) ( $p <$  0.05). Then, dual cellular staining involving cell permeable AO and only dead cell permeable EB was performed in TCS treated cells to assess the cellular morphology and fate. As shown in Fig. 1b, the cells under control condition appeared live and uniformly green in color due to the uptake of only AO dye. Here, TCS at 1 and 10  $\mu\text{M}$  concentrations showed marginal but non-significant changes as compared to control condition ( $p <$  0.05). However, a distinct impact of TCS was observed in AO stained cells at 30 and 50  $\mu\text{M}$  concentrations with significantly increased fluorescence intensity by 2.3- and 3-fold, respectively, as compared to AO stained control condition ( $p <$  0.05). Similarly, as shown in Fig. 1b, the EB stained cells also did not show any significant change at 1 and 10  $\mu\text{M}$  concentrations of TCS as compared to vehicle treated cells (control). Interestingly, the cells treated with 30 and 50  $\mu\text{M}$  concentrations of TCS showed significantly increased EB staining which was 2.4-, and 3.4-fold, respectively as compared to EB stained control condition ( $p <$  0.05) (Fig. 1b). The significant increase in EB stained cells at 50  $\mu\text{M}$  TCS treatment condition is indicative of necrosis. Based on the current data, further dose-dependent effects of TCS on Neuro-2a cells were analyzed at 10, 30 and 50  $\mu\text{M}$  concentrations.

### 3.2. TCS downregulates both autophagy and apoptosis process in Neuro-2a cells

The effect of TCS on Neuro-2a cells was investigated first at the transcription level to determine the expression pattern of apoptosis and autophagy related marker genes. In all these experiments, temsirolimus was used as a positive control, known to be an activator of autophagy (a potent inhibitor of mTOR) in neuronal cells (Boland et al., 2008).

As shown in Fig. 2a, temsirolimus increased the expression of the autophagy marker genes, LC3B) by about 1.7-fold as compared to control condition, thus confirming the induction of autophagy in these cells ( $p <$  0.05). Caspases also participate in activation and regulation of the autophagy processes (Tsapras and Nezis, 2017), and so was in our study. Temsirolimus increased the CASP8 expressions by 1.7-fold as compared to control condition ( $p <$  0.05). However, when we

**Table 1**

Details of oligonucleotide primer sequences and other details of PCR as was adopted in this study.

Name of gene	Forward Primer (5'-3')	Reverse primer (5'-3')	Annealing Temp (°C)	Product Size (BP)
LC3B (MICE) (>NM_026160.5)	CCCACCAAGATCCCAGTGAT	CCAGGAACCTGGTCTTGTTCCA	60	79
CASP8 (MICE) (>NM_009812.2)	AACATTGGGAGGCATTTCGTGC	AGAAGAGCTGTAACCTGTGGC	58.9	256
TNF- $\alpha$ (MICE) (>NM_013693.3)	CCACGTCGTAGCAAACCACC	TACAACCCATCGGCTGGCAC	61.3	126
RIPK1 (MICE) (>NM_001359997.1)	TAGTCCTTAGAGGAGGACCAGC	CCCGCCTAGGTGAGGAA	61.3	281
MLKL (MICE) (>NM_001310613.1)	GCGTTGGCCCAAATTTGACT	GGTCTTCTGCCTCGTTGACA	58.3	151
Tau (MICE) (>NM_001285455.1)	TGTCCTTCTGTCTCGCC	GCCACACGAGCTTTAAAGCCA	60.5	159
$\beta$ -Actin (MICE) (>NM_007393.5)	TCACCCACACTGTGCCCATCTACGA	CAGCGGAACCGCTCATTGCCAATGG	65.0	296

**Table 2**

List of various reagents used in immunoblot analyses.

Primary antibody	Cat. No.	Dilutions	Secondary antibody	Dilutions	Chromogen
ATG7 (MICE/RAT)	sc-376212 (Santa Cruz Biotechnology Inc., Dallas, TX, USA)	1:500	Anti-mouse	1:10,000	ECL
MAP LC3 $\beta$ (MICE/RAT)	sc-271625 (Santa Cruz Biotechnology Inc., Dallas, TX, USA)	1:500	Anti-mouse	1:10,000	ECL
p62 (HUMAN/MICE)	sc-48402 (Santa Cruz Biotechnology Inc., Dallas, TX, USA)	1:1000	Anti-mouse	1:10,000	ECL
CASP8 (HUMAN/MICE)	mAb#4927 (CST, NEB, Danvers, Massachusetts, USA)	1:1000	Anti-mouse	1:10,000	ECL
CASP3 (HUMAN/MICE)	E-AB-13815 (Elabscience, Houston, TX, USA)	1:1000	Anti-rabbit	1:10,000	ECL
TNF- $\alpha$ (HUMAN/MICE)	E-AB-40015 (Elabscience, Houston, TX, USA)	1:1000	Anti-rabbit	1:10,000	ECL
RIPK3 (MICE)	E-AB-60962 (Elabscience, Houston, TX, USA)	1:1000	Anti-rabbit	1:10,000	ECL
MLKL (HUMAN/MICE)	E-AB-61022 (Elabscience, Houston, TX, USA)	1:1000	Anti-rabbit	1:10,000	ECL
P-MLKL (Ser358) (HUMAN/MICE)	GTx00973 (GeneTex, Inc., CA, USA)	1:1000	Anti-rabbit	1:10,000	ECL
Tau (HUMAN/MICE/RAT)	GTx112981 (GeneTex, Inc., CA, USA)	1:1000	Anti-rabbit	1:10,000	ECL
P-Tau (Ser198) (HUMAN/MICE/RAT)	GTx130456 (GeneTex, Inc., CA, USA)	1:1000	Anti-rabbit	1:10,000	ECL
$\beta$ -Actin (MICE)	sc-47778 (Santa Cruz Biotechnology Inc., Dallas, TX, USA)	1:1000	Anti-mouse	1:10,000	ECL

Clarity Western ECL blotting substrate (Cat. No. 17506061; Bio-Rad Laboratories, Inc., Hercules, California, USA) was used as chromogen.

tested for TCS, it was found to inhibit autophagy marker gene almost in a dose-dependent manner. At 50  $\mu$ M concentration of TCS the expression of LC3B was inhibited by about 2.3-fold as compared to control condition (Fig. 2a) ( $p < 0.05$ ). With the decrease in autophagy marker gene, there were a subsequent decrease in CASP8 expression by about 1.7-fold in response to 50  $\mu$ M concentration of TCS as compared to control condition ( $p < 0.05$ ) (Fig. 2a). Next, we measured the expression of three distinct autophagy markers at the translational level in response to TCS. As shown in Fig. 2b, temsirolimus induced ATG7 and LC3B expression by about 1.6- and 1.7-fold, respectively, with a subsequent decrease in p62 levels by about 2.7-fold ( $p < 0.05$ ), a typical pattern of autophagy marker expressions during active autophagy process. p62 is a membrane protein whose downregulation confirms generation of autophagic flux and formation of autophagolysosomes (Galluzzi et al., 2012), thus, indicating proper induction of autophagic process in the cells. On the contrary, TCS inhibited the normal autophagic process in the cells in a dose dependent manner, albeit at varying levels of significances. As shown in Fig. 2b, TCS at 50  $\mu$ M concentration downregulated ATG7 and LC3B expression by about 1.5 and 3.7-fold, respectively, with subsequent induction of p62 expression by about 1.9-fold as compared to control condition ( $p < 0.05$ ). Taken together, all these data suggested that TCS was inhibiting the autophagy in the cells at the same time inducing cellular damage not by causing apoptosis but by some other mechanisms, thus warranting further analysis.

### 3.3. TCS persuades autophagy vacuoles formation but unable to induce flux in Neuro-2a cells

To further investigate the potent inhibition of autophagy-associated proteins in Neuro-2a cells in presence of TCS, the cellular staining experiments justifying the generation of autophagic vacuoles and formation of autophagolysosomes were performed. The abrupt induction of autophagy is considered as a hallmark of neurodegenerative disease (Heras-Sandoval et al., 2014). The presence of autophagic vacuole is a characteristic feature of autophagy. In

order to confirm this, in our subsequent study, we examined the generation of autophagic vacuole in Neuro-2a cells by MDC staining. MDC dye is used as a tracer for autophagic vacuole localization and makes them distinctly visible. As shown in Fig. 3a, the control cells did not show any indication of MDC dye stained cells, whereas the treatment of cells with autophagy-inducer temsirolimus (0.2  $\mu$ M) resulted in an increase in MDC stained cells by about 2.5-fold as compared to control ( $p < 0.05$ ), which confirmed the formation of autophagic vacuoles. Further it is also evident from Fig. 3a that at a higher concentration of TCS (50  $\mu$ M), a significant increase in the MDC-stained cells was observed, albeit at a lesser level as compared to temsirolimus, thus confirming the formation of autophagic vacuoles.

In order to further validate the aggregation of autophagic vacuoles in cells, EGFP-LC3 puncta formation was analyzed under different treatment conditions. Lipidation of autophagic vacuoles is a hallmark of mature autophagosomes, which further fuses with active lysosomes, thus ultimately forming autophagolysosomes (Varshney et al., 2017). Up-regulated p62, together with endogenous LC3B even at low expression, is a precursor for autophagy puncta formation (Runwal et al., 2019). As shown in Fig. 3b, the treatment of EGFP-LC3 transfected cells with temsirolimus resulted in distinct punctuated dots in its cytoplasm which was almost 3-fold higher than the control condition ( $p < 0.05$ ), indicative of LC3B puncta formation, a prerequisite condition for autophagic process. However, treatment of EGFP-LC3B transfected Neuro-2a cells with TCS did not lead to the formation of any punctuated dots at lower concentration, although punctuate dots were visible at 50  $\mu$ M concentration which was almost at the same level (3-fold) as that of temsirolimus treated cells ( $p < 0.05$ ) (Fig. 3b). This could be attributed to the fact as discussed earlier that at low level of expression of LC3 gene, it can form autophagy-like aggregates along with overexpressed p62 protein, which ultimately behaves like autophagic vacuoles. However, further detailed studies are needed using better autophagic markers and inducers to elucidate the exact cross-talks between triclosan and autophagy process in these cells. This is one of the limitations of our current study.

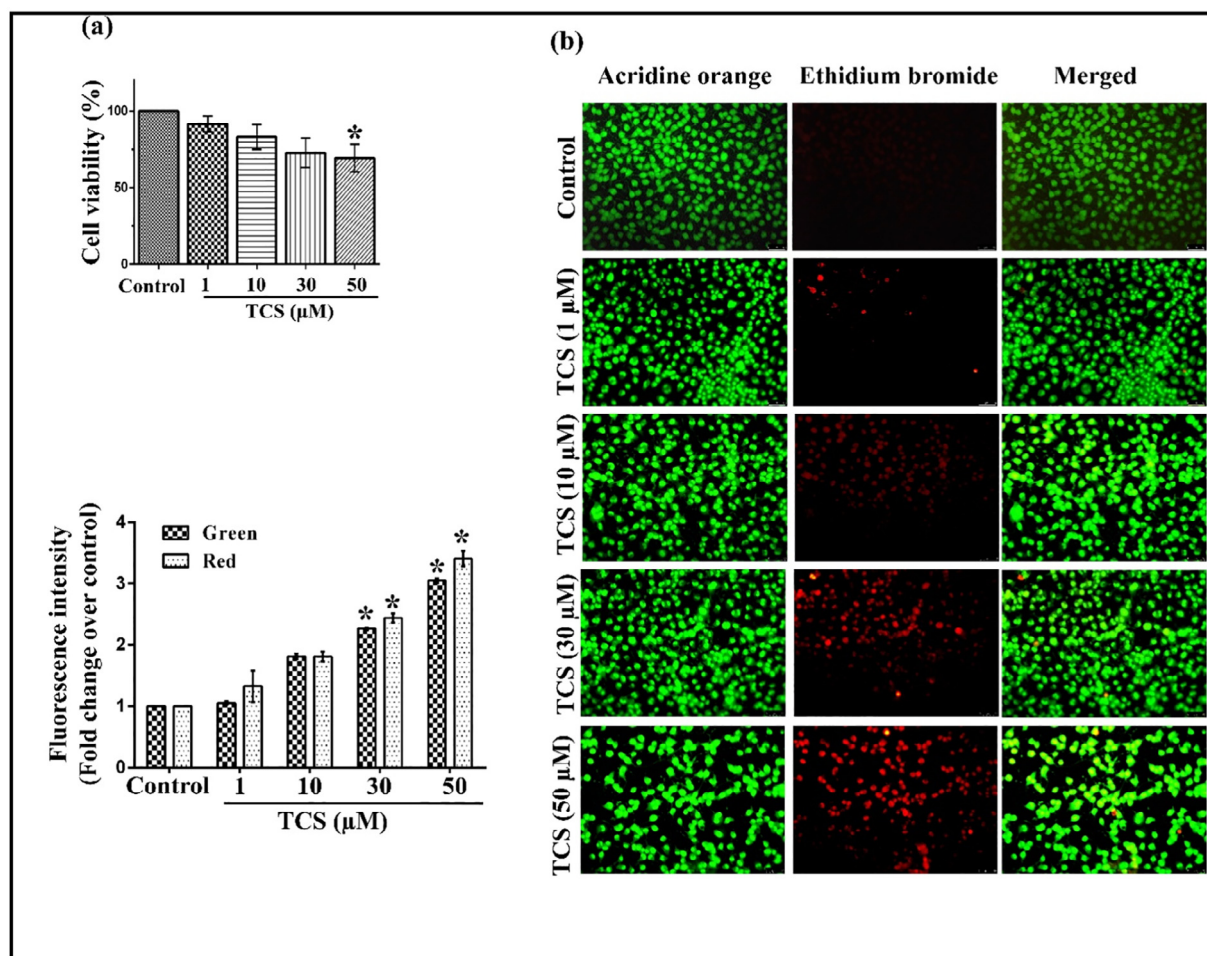


**Fig. 1.** Effect of TCS on Neuro-2a cell viability and morphology. The cells were treated with varying concentration of TCS (1, 10, 30 and 50  $\mu\text{M}$ ) for 24 h. DMSO treated cells were considered as control. (a) MTT assay was performed to evaluate the viability of cells. The result is considered as mean  $\pm$  SEM. of three independent experiments. \* represents  $p < 0.05$  as compared with the vehicle-treated control group, which was considered 100% viable. (b) Representative acridine orange/ethidium bromide dual staining images of the cells after TCS treatment. The magnification and scale bar for (b) are 200 $\times$  and 50  $\mu\text{m}$  respectively. The histogram shows the quantification of images in (b) using ImageJ software. Data are mean  $\pm$  SEM of three independent experiment. TCS, triclosan. (For interpretation of the references to color in this figure legend, the reader is referred to the web version of this article.)

The observed inability to generate autophagy flux was further assessed by lysotracker assay to estimate the formation of autophagolysosomes. Neuro-2a cells, treated under previously mentioned conditions, were stained with lysotracker (DND99) red, a fluorescent dye, which precisely labels the cellular acidic cargos, such as late endosomes and active lysosomes (Pierzyńska-Mach et al., 2014). The viability of cells was confirmed by counterstaining the cells with AO dye. As shown in Fig. 4, the treatment of Neuro-2a cells with autophagy inducer, temsirolimus (0.2  $\mu\text{M}$ ), resulted in the appearance of active lysosomes confirming the formation of active autophagolysosomes, as visualized by DND99 red staining, which was otherwise absent in control condition. It was observed that increasing concentration of TCS did not support the active lysosome formation, as confirmed by the absence of DND99 red-stained cells. Altogether, these results confirmed that TCS prevents autophagy flux generation and inhibits autophagosome fusion to lysosomes, thus wholly abrogating the autophagic process in Neuro-2a cells. Some earlier genetic and functional studies indicated that autophagy is an anti-inflammatory process that affects numerous pathways (Deretic et al., 2013). Based on this information in the next part of the study we proceeded to explore if TCS resulted in any neuroinflammatory responses in Neuro-2a cells.

#### 3.4. TCS generates loss in mitochondrial integrity in Neuro-2a cells

TCS has been reported to induce metabolic acidosis in cells (Zheng et al., 2019). Thus, its impact on mitochondrial membrane potential ( $\Delta\psi\text{m}$ ) of Neuro-2a cells was investigated. JC-1 is a membrane permeant fluorescent probe, which remains in a healthy cell as aggregate. A depolarization of  $\Delta\psi\text{m}$  from  $>150$  mV to  $<101$  mV in an affected cell causes conversion of JC-1 aggregates into monomer units and results in shift of fluorescent emission from red to green. CCCP is a potent mitochondrial uncoupler which causes a shift from red to green fluorescence. As evidenced in Fig. 5, 30 and 50  $\mu\text{M}$  concentration of TCS resulted in shift from red to green fluorescence in Neuro-2a cells, which confirms the loss in the  $\Delta\psi\text{m}$ . As shown in bar graph, the cells treated with CCCP resulted in about 8-fold increase in green fluorescence monomer with subsequent decrease in red fluorescence dimers by about 7.7-fold as compared to respective (green and red) control groups ( $p < 0.05$ ). Interestingly, 30 and 50  $\mu\text{M}$  concentrations of TCS respectively led to significant change in green fluorescence monomer with almost 1.9- and 2.1-fold increase, while the red fluorescence dimers were significantly decreased by about 3.5- and 3.7-fold as compared with respective control condition ( $p < 0.05$ ). In TCS 10  $\mu\text{M}$  concentration a marginal but non-significant change was observed in

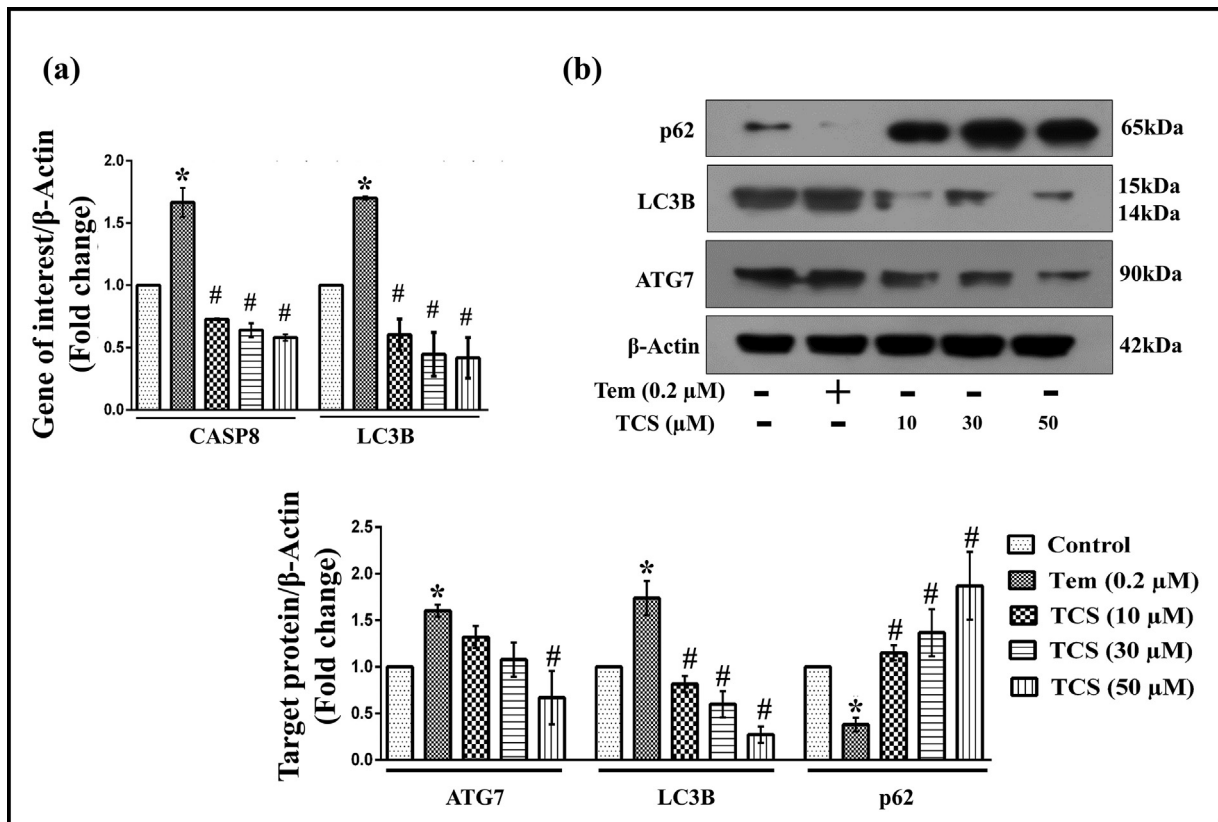


**Fig. 2.** Effect of TCS on transcription and translation of apoptosis and autophagy associated markers in Neuro-2a cells. The cells were treated with DMSO (control), 0.2 μM temsirolimus (positive control), and TCS (10, 30 and 50 μM) for 24 h. (a) Bar graph illustrating RT-qPCR analysis for the relative quantification of mRNA expression of respective genes. (b) Representative expression pattern of autophagy related proteins (ATG7, LC3B and p62) as determined by immunoblot analysis. β-Actin was used as internal control in all analyses. The bar graphs in (a) and (b) represents fold change in expression as compared to vehicle treated control cells in respective groups. Results are representative of three independent experiments with mean ± SEM. \* and # indicate  $p < 0.05$  as compared to vehicle and temsirolimus treated cells, respectively for respective genes or proteins. TCS, triclosan; Tem, temsirolimus.

green and red fluorescence monomers and dimers respectively as compared to control cells ( $p < 0.05$ ). Above results suggests that TCS hampers the integrity of mitochondria by disrupting mitochondrial membrane potential in Neuro-2a cells.

### 3.5. TCS initiates TNF-α signaling pathway associated necroptosis in Neuro-2a cells

The loss of autophagy flux and inhibition of apoptosis may lead to activation of caspase-independent inflammatory pathway governed by necroptosis. Necroptosis is a programmed form of necrotic death which is dependent on Tumor Necrosis Factor-α (TNF-α) governed activation and simultaneous interaction of Receptor-interacting serine/threonine-protein kinases (RIPK1, RIPK3) and Mixed Lineage Kinase domain Like pseudokinase (MLKL) proteins (Murphy et al., 2013). The chromosomal DNA integrity was assessed by performing DNA fragmentation analysis after isolating total cellular DNA from TCS treated Neuro-2a cells. A differential DNA pattern was observed in agarose gel electrophoresis analysis of the total DNA extracted from TCS treated Neuro-2a cells as compared to control condition. TCS induced the DNA cleavage at lower concentrations (1 and 10 μM) with appearance of ladder formation, a marker of induction of apoptosis (Fig. 6a). Interestingly, the treatment at 50 μM TCS concentration resulted in appearance of DNA smear without any significant ladder formation (Fig. 6a). The downregulation in CASP8 expression (Fig. 2a), increase in necrotic cells (Fig. 2b) and appearance of smear formation (Fig. 6a) led us to investigate the expression of the necroptosis-associated markers. The expression of TNF-α and MLKL genes was further validated by performing quantitative RT-qPCR. As

evident from Fig. 6b, the expression of both TNF-α and MLKL were increased by about 3.7- and 5.7-fold, respectively, at 50 μM TCS treatment condition, as compared to control condition ( $p < 0.05$ ). These genes are responsible for programmed necrotic cell death, i.e., necroptosis.

In order to further ascertain the impact of TCS on activation of necroptosis pathway, the protein levels of the above-mentioned genes were determined by immunoblot analysis. As shown in Fig. 6c, the expression of TNF-α was found to be upregulated by 6.6-fold in response to 50 μM concentration of TCS ( $p < 0.05$ ). Interestingly, the expression of apoptosis-related proteins, namely CASP8 and CASP3, were found to be downregulated by about 2.8- and 3.1-fold, respectively, in response to 50 μM TCS treatment with respect to control condition (Fig. 6c) ( $p < 0.05$ ). The expression of neuroinflammatory intermediate marker, RIPK3, was found to be upregulated by 10.4-fold of 50 μM TCS as compared to control condition (Fig. 6c) ( $p < 0.05$ ). MLKL acts as a major executioner protein, which ruptures the plasma membrane and ultimately leads to cell death. RIPK1 and RIPK3 dependent necrosome formation further enhance the recruitment and concomitant phosphorylation of MLKL protein in the cells (Pasparakis and Vandennebe, 2015). As expected, the expression of MLKL and p-MLKL was also found to be upregulated by 5- and 5.9-fold, respectively, in response to 50 μM TCS treatment (Fig. 6c) ( $p < 0.05$ ). The increased expression of these proteins leads to their simultaneous interaction and cross-phosphorylation, which generally form the necrosome (Frank et al., 2019; Mandelkew and Mandelkew, 1998). Taken together, these results strongly suggested that TCS induced the activation of necroptosis pathway by generating inflammatory responses in the Neuro-2a cells.

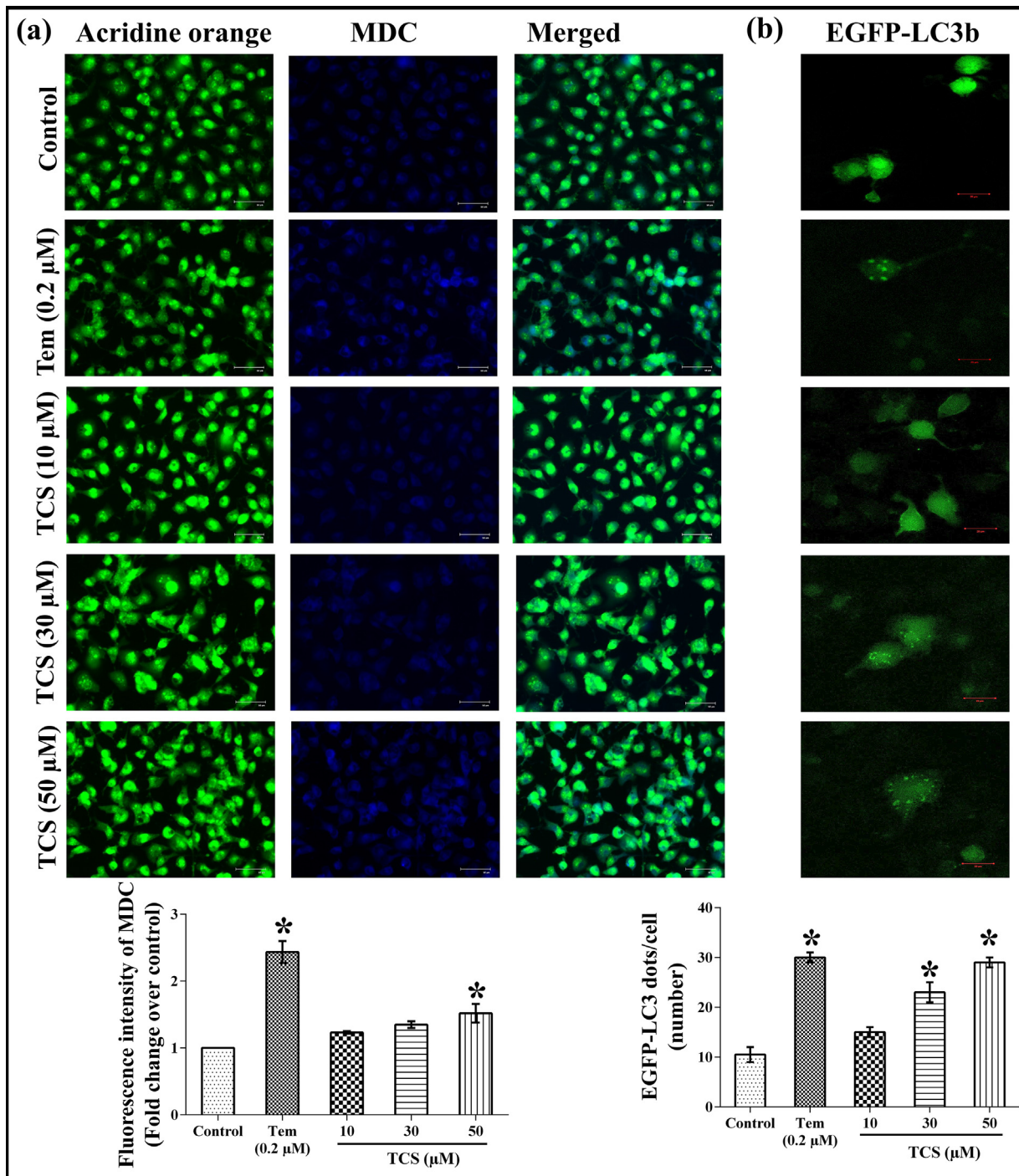


**Fig. 3.** Effect of TCS on the accumulation of autophagic vacuoles in Neuro-2a cells. The cells were treated with DMSO (control), 0.2 μM temsirolimus (positive control), and TCS (10, 30 and 50 μM) for 24 h. (a) Representative fluorescence microscopy images to show the formation of autophagic vacuoles in cells by staining with MDC. The images were captured at 200× magnification (scale bar, 58 μm). (b) Representative confocal microscopy images depicting EGFP-LC3 puncta formation in response to various treatment conditions. The images were captured at 630× magnification (scale bar, 20 μm). The bar graph below respective figures in (a) and (b) indicates the quantification of the respective images performed with the use of ImageJ software. Results are representative of three independent experiments with mean ± SEM. \* indicates  $p < 0.05$  as compared to vehicle treated control. TCS, triclosan; Tem, temsirolimus; MDC, monodansylcadaverine.

### 3.6. Necroptosis inhibitor attenuates necroptosis in TCS treated Neuro-2a cells

Necrostatin-1 (Nec-1) is a small molecule inhibitor of RIPK1 that specifically inhibits phosphorylation of RIPK1 and RIPK1-mediated necroptosis (Galluzzi et al., 2012). Thus, to further validate the

necroptotic effect of TCS in Neuro-2a cells, we compared the expression pattern of associated MLKL protein in Neuro-2a cells under different treatment conditions by immunoblot analyses. Similar to the above-mentioned results, 50 μM concentration of TCS increased the MLKL expression by 4.2-fold as compared to control condition (Fig. 7) ( $p < 0.05$ ). However, MLKL expression remained unaltered

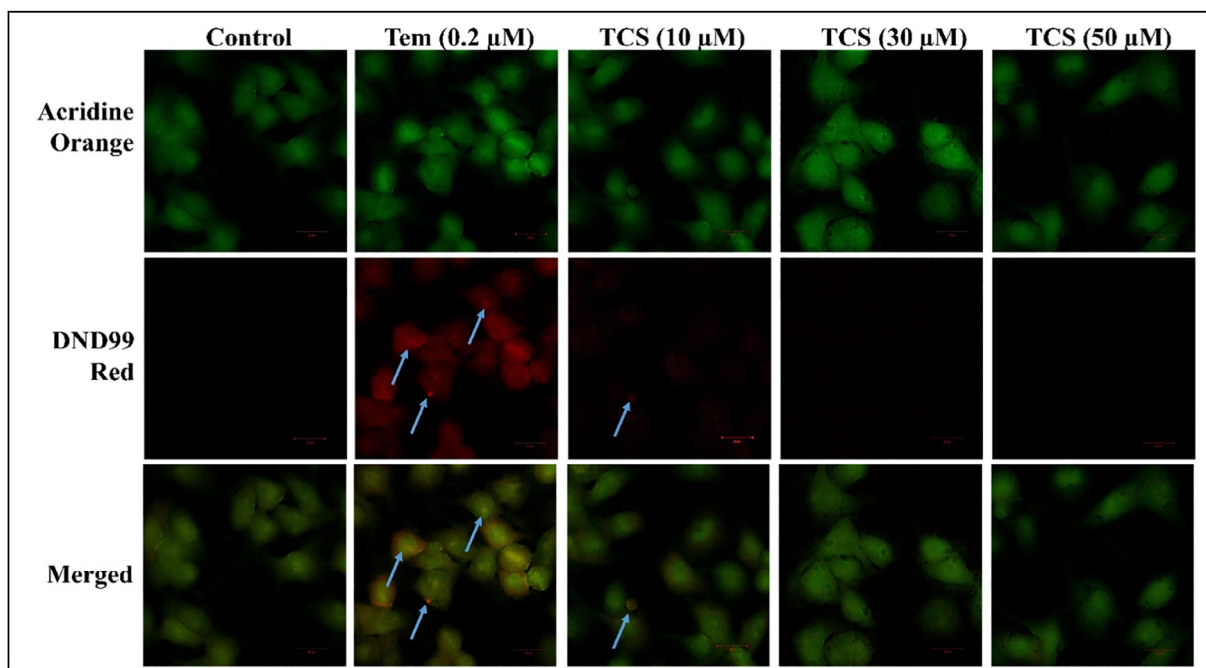


**Fig. 4.** Effect of TCS in the formation of active lysosomes in Neuro-2a cells. The cells were treated with DMSO (control), 0.2 μM temsirolimus (positive control), TCS (10, 30 and 50 μM) for 24 h. Representative confocal microscopic images to show the formation of autophagolysosomes in cells by staining with lysotracker DND99 red stain. Blue arrows indicate the presence of active autophagolysosomes in cells. The images were captured at 630 × magnification (scale bar, 20 μm). All experiments were performed three times independently. TCS, triclosan; Tem, temsirolimus. (For interpretation of the references to color in this figure legend, the reader is referred to the web version of this article.)

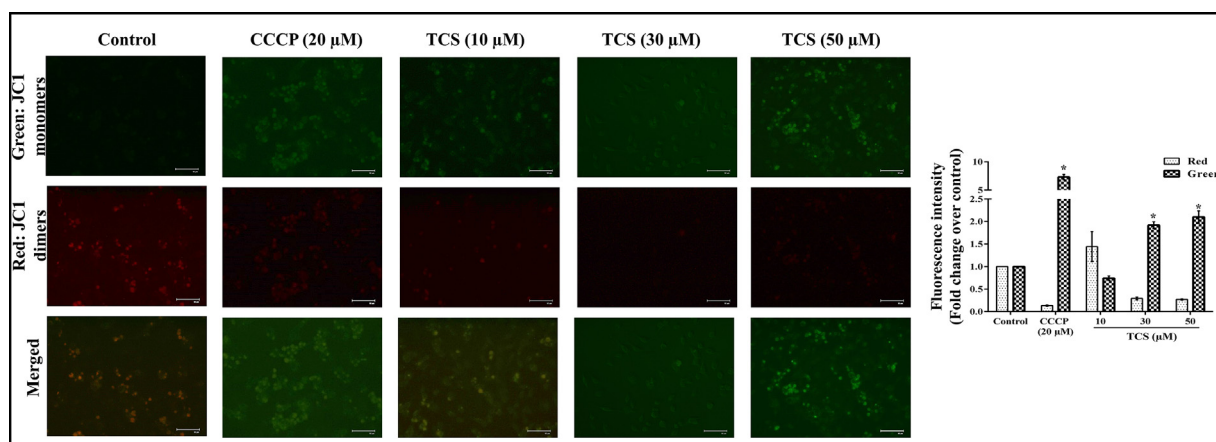


**Fig. 5.** Effect of TCS on mitochondrial membrane potential in Neuro-2a cells. The cells were treated with DMSO (control), CCCP (positive control), and TCS (10, 30 and 50 μM) for 24 h. Representative fluorescent microscopic image showing the loss of mitochondrial membrane potential in cells stained with JC-1 fluorescent probe. The images were captured at 200x magnification (scale bar, 92 μm). All experiments were performed three times independently and image quantification was performed with the help of ImageJ software with mean ± SEM and shown as bar graph. \* indicates  $p < 0.05$  as compared to control cells in green fluorescent group. TCS, triclosan; CCCP, carbonyl cyanide 3-chlorophenylhydrazone.

after Nec-1 treatment and was almost at the same level as control condition (Fig. 7). Thereafter, we also determined the MLKL expression in cells under TCS (50 μM) and Nec-1 (0.1 μM) co-treatment condition, and as shown in Fig. 7, TCS induced upregulation of MLKL was significantly blunted by Nec-1 ( $p < 0.05$ ). This data further indicated that TCS needs the active participation of necroptosis pathway to show its deleterious effects in neuronal cells.

Since Nec-1 masked the necroptotic effect of TCS in cells, the expression of upstream marker CASP8 protein was also analyzed to determine the cell fate in co-treatment condition. CASP8 concurrently acts as inhibitor of necroptosis and initiator of extrinsic apoptosis

(Chen et al., 2018). TCS (50 μM) downregulated the CASP8 expression by 2-fold as compared to control condition ( $p < 0.05$ ) (Fig. 7). On the contrary, in the presence of Nec-1, the inhibition of TCS-induced CASP8 was reversed, and an increase in expression was observed by about 2.1-fold as compared to only TCS treated condition ( $p < 0.05$ ) (Fig. 7). To further confirm the activation of apoptotic cell fate, the expression pattern of executioner CASP3 protein was also analyzed and as shown in Fig. 7, a 2.3-fold upregulation of CASP3 expression was observed in TCS and Nec-1 co-treatment condition as compared to only TCS treated cells ( $p < 0.05$ ). This data further confirmed that once the necroptotic pathway was blocked, TCS might induce caspase

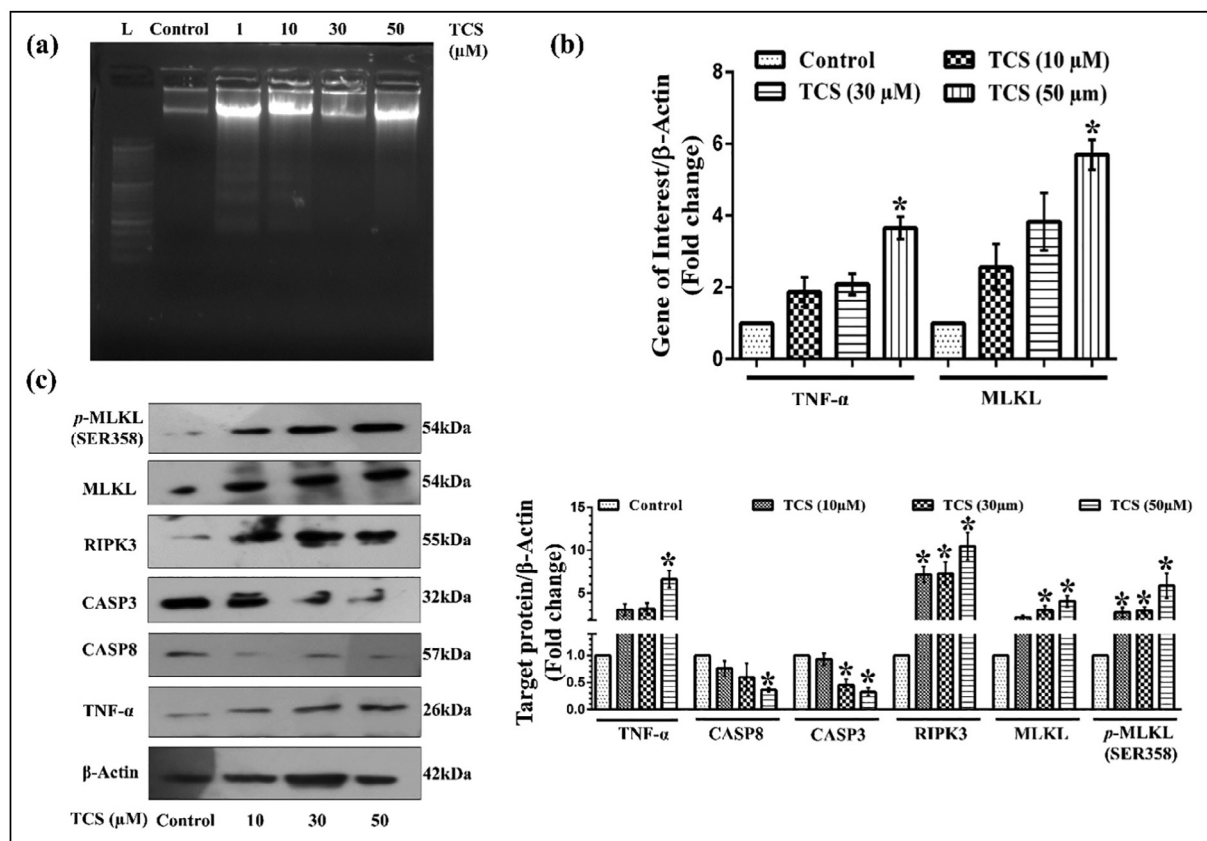


**Fig. 6.** Effect of TCS on the expression of necroptosis associated marker genes in Neuro-2a cells. The cells were treated with DMSO (control), and TCS (10, 30 and 50  $\mu$ M) for 24 h. (a) Representative gel image displaying the formation of DNA ladder or smear in response to TCS. (b) Bar graph illustrating RT-qPCR analysis for the relative quantification of mRNA expression for indicated genes. (c) Representative expression pattern of necroptosis associated proteins as determined by immunoblot analysis.  $\beta$ -Actin was used as internal control in all analyses. The bar graphs in (b) and (c) represents fold change in expressions as compared to control cells for respective genes (b) or proteins (c). Results are representative of three independent experiments with mean  $\pm$  SEM. \* indicates  $p < 0.05$  as compared to control cells in respective genes (b) or proteins (c). TCS, triclosan.

dependent pathway. Surprisingly in our study Nec-1 was also found to marginally upregulate the expressions of both CASP3 and CASP8, albeit at varying levels. Although this does not interfere much with the interpretation of the current data, but it definitely demands further detailed analysis which is another short coming of this study. Collectively, these findings further validated the necroptosis inducing nature of TCS in Neuro-2a cells. However, in presence of necroptosis inhibitor (Nec-1) TCS alienated the Neuro-2a cells to apoptotic fate.

### 3.7. TCS induces necroptosis-mediated tau pathogenesis in Neuro-2a cells

The increased expression of RIPK1, RIPK3 and MLKL and their phosphorylated forms generate the necrosomes in the cells, which ultimately leads to the onset of Alzheimer's disease. Alzheimer's disease is associated with changes in the basal tau protein level and its posttranslational modifications, namely increased phosphorylation and truncation (Mandelkow and Mandelkow, 1998; Muralidar et al., 2020). To elucidate the effect of TCS on tau expression in Neuro-2a cells, transcriptional and translational analyses were performed. The quantitative RT-qPCR (Fig. 8a) analysis revealed that TCS increased the tau gene expression to maximum of 3-fold at 50  $\mu$ M TCS concentration as compared to control condition ( $p < 0.05$ ).

To further ascertain the tau pathogenesis effect of TCS, the expression of tau protein and its phosphorylated form (p-tau) were analyzed by immunoblot analysis. As shown in Fig. 8b, the expression of tau protein increased dose dependently with increasing concentration of TCS and at 50  $\mu$ M concentration, it was upregulated by about

3.2-fold as compared to control condition ( $p < 0.05$ ). When checked for the phosphorylated levels of tau protein, TCS was found to enhance the expression level of p-tau protein, which was about 1.6- and 2.2-fold at 30 and 50  $\mu$ M treatment concentrations in Neuro-2a cells, respectively as compared to control condition ( $p < 0.05$ ) (Fig. 8b). However, the phosphorylation of tau protein was not found to increase concomitantly with increase in the tau protein level in respective TCS treatment condition. This aspect of phosphorylation of tau protein therefore needs to be addressed and validated further with better control and experimental set up which remained as a gap in this study. However, together the current data confirmed the pathogenesis of tau protein and alluded to the probable progression of tau-aggregated neurodegeneration in TCS treated neuronal cells.

## 4. Discussion

There are several reports involving different *in vitro* studies that showed TCS imparted deleterious effect on the viability and morphology of neuronal cells. In multicellular organisms, the cellular fate in presence of foreign pathogen, toxicant or injury depends on three classical phenomena, namely, autophagy, apoptosis and necrosis, which may act independently or associatively (Chen et al., 2018). Inflated oxidative stress in the mitochondria results in damage and a loss of mitochondrial membrane potential, which eventually leads to pore development. TCS generates a protonophoric response in Neuro-2a cells, which results in loss of mitochondrial membrane potential. Autophagy is lysosome-dependent cell survival pathway that maintain

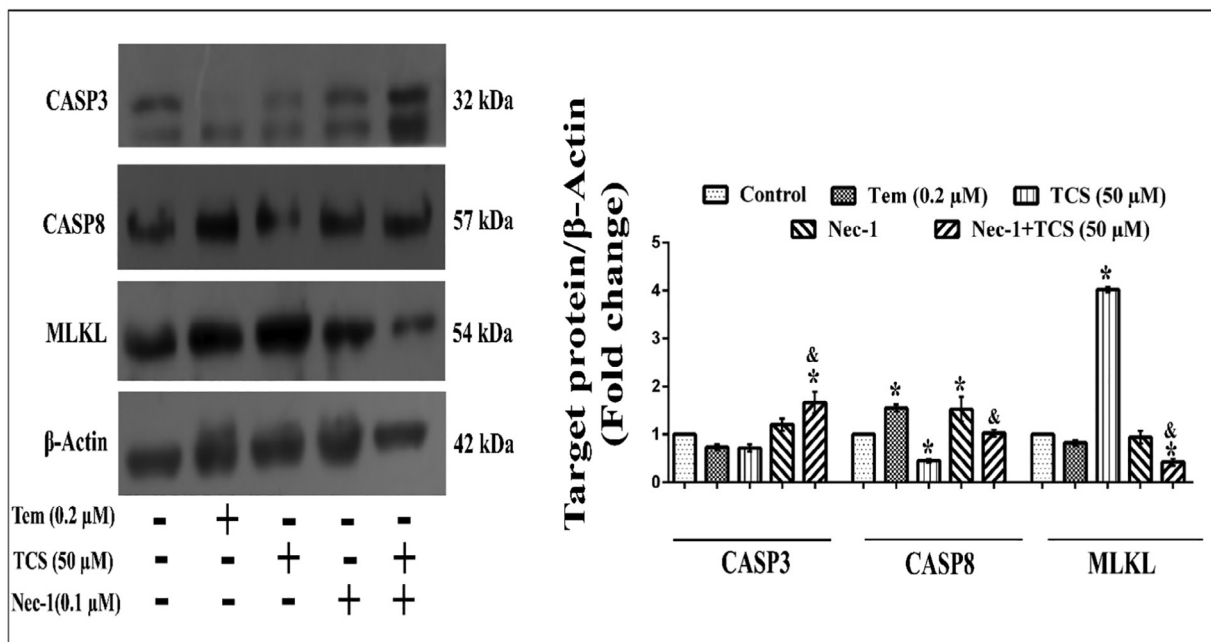


**Fig. 7.** Comparative analysis of translational pattern of necroptosis associated proteins in presence of necrostatin-1 in Neuro-2a cells. Representative immunoblot analysis indicating the expression level of necroptosis associated proteins (CASP8, CASP3 and MLKL) under various treatment conditions.  $\beta$ -Actin was used as internal control in all analyses. The adjacent bar graph represents fold change in expression as compared to control cells in respective proteins. Results are representative of three independent experiments with mean  $\pm$  SEM. \* and & indicates  $p < 0.05$  as compared to control cells and temsirolimus treated cells respectively for respective proteins. TCS, triclosan; Tem, temsirolimus; Nec-1, necrostatin-1.

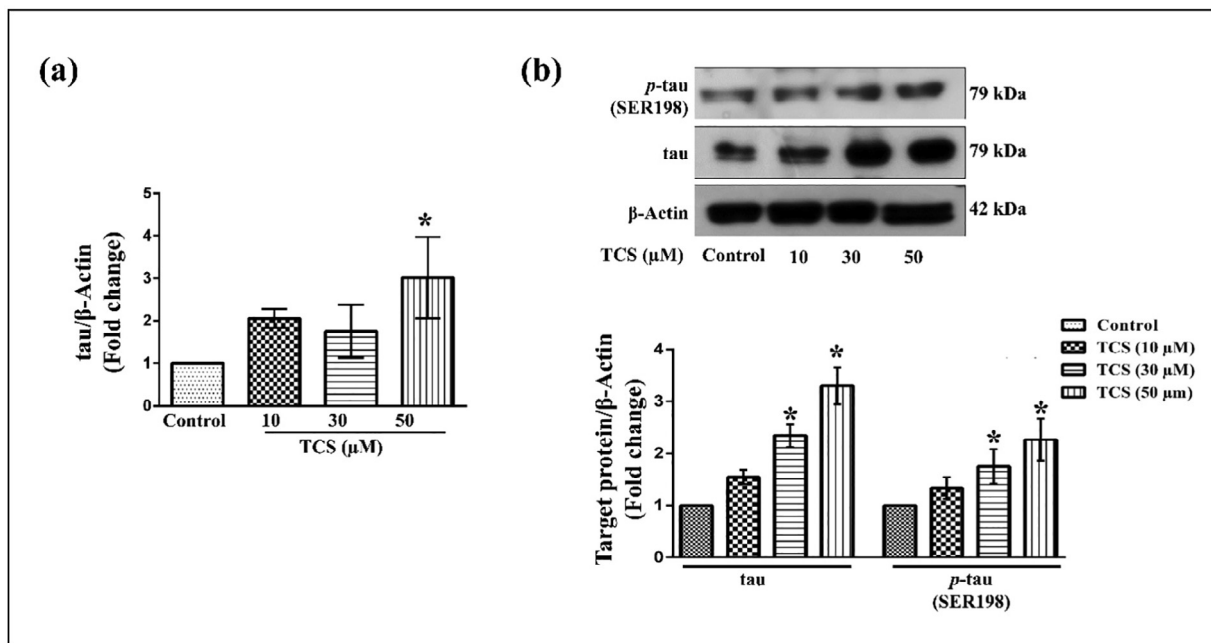


**Fig. 8.** Effect of TCS on the expression of tau protein in Neuro-2a cells. The cells were treated with DMSO (control) and TCS (10, 30 and 50  $\mu$ M) for 24 h. (a) Bar graph illustrating RT-qPCR analysis for the relative quantification of tau gene transcription. (b) Representative expression pattern of tau and  $p$ -tau proteins as determined by immunoblot analysis.  $\beta$ -Actin was used as internal control in all analyses. The respective bar graphs in (a) and (b) represent the fold change in expression as compared to control cells in respective genes or proteins, respectively. Results are representative of three independent experiments with mean  $\pm$  SEM. \* indicates  $p < 0.05$  as compared to control cells in respective genes or proteins. TCS, triclosan.

the homeostasis of cells by clearing misfolded and abnormal proteins through selective degradation. However, it may also induce cell death in certain instances (Boland et al., 2008; Nixon, 2013). Temsirolimus, a recently approved drug for the treatment of renal cell carcinoma by

the U.S. Food and Drug Administration (FDA) and European Medicines Agency (EMA), is a positive inducer of autophagy. Temsirolimus initiates the formation of autophagic vacuole in neuronal cells, and after activating pivotal autophagy-related proteins, it merges autophago-

somes with acidic lysosome and completes the process of autophagy (Jiang et al., 2014). TCS, although induced the formation of autophagic vacuole in neuronal cells, but it does not effectively execute the entire autophagic process. This behavior can be interpreted by the fact that downregulation of pivotal protein LC3B, responsible for lipidation of the bilayer membrane, leads to the closure of autophagosomes, and activation of LC3B complex, respectively. In the current study we highlighted the involvement of LC3B as autophagy marker in response to TCS. Subsequently, the failure in generation of autophagy flux results in the lack of fusion of autophagosome to lysosome. p62 is an autophagy associated membrane protein whose level in a cell decreases with the formation of autophagolysosome. In absence of the fusion of autophagosome and lysosome (autophagolysosome formation) the level of p62 is increased throughout the cells. In our study the increased expression of p62 proteins with increase in TCS concentration in neuronal cells further established disruption in the formation of autophagolysosomes, thus confirming failure in execution of autophagy which was in accordance to some earlier reports (Runwal et al., 2019).

Apoptosis, a caspase-dependent programmed cell death, involves either CASP8-associated-death-receptor-mediated apoptosis or CASP9-associated-mitochondria-dependent apoptosis (Elmore, 2007; Yuan and Yankner, 2000). The downregulated expressions of CASP8 in our study confirmed that TCS did not induce apoptosis in neuronal cells. Defective autophagy cannot clear the abnormal and toxic proteins, whose accumulation leads to neurological disorders (Heras-Sandoval et al., 2014). The inhibition in the generation of effective autophagy flux, along with downregulated CASP8 expression, has been correlated to increased expression of MLKL protein, which promotes TNF- $\alpha$  based necroptosis (Pasparakis and Vandenabeele, 2015). Inflammation is associated with increased expression of pro-inflammatory cytokines and inducing oxidative stress. Free radicals, mainly reactive oxygen species (ROS) and reactive nitrogen species (RNS), production increases exponentially on exposure to inflammatory conditions (Mittal et al., 2014; Wang et al., 2019). TCS has been previously reported to increase ROS production in cells (Szychowski et al., 2020).

Our study demonstrated the TCS persuaded necroptosis involving TNF- $\alpha$  signaling pathway. TNF- $\alpha$  is a pleiotropic cytokine that generates a complex with RIPK1 and plays an imperative role in the progression of inflammation. The inhibition of this complex formation is dependent on increased expression of another complex, consisting of CASP8 and FADD proteins, which cleaves the RIPK1 protein (Tait and Green, 2008). The downregulated CASP8 expression in Neuro-2a cells prevented the cleavage of RIPK1, which further allowed the trans-phosphorylation of RIPK1 and RIPK3 proteins. The enhanced level of phosphorylated form of these proteins increased the expressions of both MLKL and p-MLKL proteins (Chen et al., 2018). Some of the earlier studies confirmed that the upregulation in the expression of these cascades of proteins generates another complex in the cells, which leads to the disintegration of plasma membrane and leakage of cellular contents (Budd et al., 2006; Li et al., 2006). Necrostatin-1 (Nec-1) is a chemical compound that inhibits RIPK1 activity to further block necroptosis cascade (Galluzzi et al., 2012). It was observed that the blockage of RIPK1 expression by Nec-1 in Neuro-2a cells further attenuated the downstream necroptosis regulatory marker, MLKL. CASP8 is a crucial mediator molecule involved in the apoptosis and necroptosis pathway (Pasparakis and Vandenabeele, 2015; Tait and Green, 2008). The downregulated expression of CASP8 in Neuro-2a cells in the presence of TCS allowed the increased expression of necroptotic proteins, namely RIPK1, RIPK3 and MLKL.

The failure of autophagy execution and generation of neuroinflammation in Neuro-2a cells suggested the neurodegenerative property of TCS. The repression of fusion of autophagosomes and lysosomes is considered as the hallmark of neurological disorders and the autophagic dysfunction in the CNS has been shown to cause Alzheimer's

disease (Kuboyama et al., 2006). The link between the lack of autophagy in neuronal cells and enhanced probability of neurological disorder could be attributed to the fact that in the absence of autophagy there is heavy accumulation of defective and/or degenerative proteins within cells. This leads to malfunctioning of several cellular activities, which are cleared off by the autophagic process in normal condition. The microtubule-associated protein, tau, regulates the polymerization, stabilization and assembly of axonal microtubules (Wander et al., 2020; Vogel et al., 2021). Many studies have reported tauopathies, as indicated by misfolding, mislocalization and hyperphosphorylation of tau proteins, are responsible for causing Alzheimer's disease (Berger et al., 2007; Muralidar et al., 2020). This could also be associated with autophagy because with an active autophagic process in a cell; this defective tau protein could be eliminated, thus reducing its accumulation within cells. Our study revealed that TCS enhanced the level of total tau protein along with marginal phosphorylation of tau protein. Possibly this might be responsible for causing tau-associated neurodegeneration in long run as has been reported in earlier studies where tau-induced pathogenesis and associated neuroinflammation was induced due to the accumulation of total tau protein with its minimal phosphorylation. It has recently been reported that total tau aggregation is more prone to hypo- to hyper-phosphorylation in the brain of Alzheimer patients, and tau cluster formation is induced by a neuroinflammatory response (Wander et al., 2020; Vogel et al., 2021). This could again be correlated with inhibition of autophagy by TCS because normal autophagy within these cells might have reduced the levels of enhanced phosphorylated tau protein, thus protecting them from getting damaged. However, this aspect needs further detailed analysis substantiated by experimental evidences to draw a confirmed conclusion.

## 5. Conclusions

The present study elucidates the neuroinflammatory potential of TCS in Neuro-2a cells. TCS's protonophoric potential induces mitochondrial damage, which leads to neuroinflammation. Further, our study confirmed that TCS initiates caspase-independent cell death through activation of TNF- $\alpha$  signaling pathway. The abrogated autophagy induces the overexpression of p62 which further causes neuroinflammation leading to tau-mediated neurodegeneration. Conclusively, this study defines the crosstalk between the autophagy, apoptosis, and necroptosis executed by the prime mediator CASP8. Overall, this study provides some preliminary information regarding the neuroinflammatory potential of bioaccumulated TCS. Therefore, there is an exclusive need for a detailed study involving appropriate *in vitro* and *in vivo* experimental models to confirm further the exact role of this chemical as an agent causing neurodegeneration. Based on these data, a complete neurotoxic profile of TCS could be drawn, which would help the policymakers to decide the appropriate dosages of its usage in various day-to-day materials.

## Declarations

**Funding**, This work is supported by a research fellowship (JRF/SRF) and contingency assistance from the Council for Scientific and Industrial Research (CSIR), Government of India to PK.

**Conflicts of interest**, The authors declare that they have no conflicts of interest.

**Contributions**, PK and PR designed the entire study. PK completed the experiment process, literature search and generation of figures. SB and SN provided support in experimentation. PK and PR wrote the manuscript while SB and SN supported in editing the manuscript. All authors read and approved the final manuscript.

**Ethics declarations**, Not applicable.

**Consent for publication**, Not applicable.

## Ethics approval and consent to participate, Not applicable.

## Declaration of Competing Interest

The authors declare that they have no known competing financial interests or personal relationships that could have appeared to influence the work reported in this paper.

## References

- Arias-cavieles, A., More, J., Vicente, J.M., Adasme, T., Hidalgo, J., Valdés, J.L., Humeres, A., Valdés-undurraga, I., Sánchez, G., Hidalgo, C., Barrientos, G., 2018. Triclosan impairs hippocampal synaptic plasticity and spatial memory in male rats. *Front. Mol. Sci.* 11, 1–13. <https://doi.org/10.3389/fmol.2018.00429>.
- Bedoux, G., Roig, B., Thomas, O., Dupont, V., Le Bot, B., 2012. Occurrence and toxicity of antimicrobial triclosan and by-products in the environment. *Environ. Sci. Pollut. Res.* 19, 1044–1065. <https://doi.org/10.1007/s11356-011-0632-z>.
- Berger, Z., Roder, H., Hanna, A., Carlson, A., Rangachari, V., Yue, M., Wszolek, Z., Ashe, K., Knight, J., Dickson, D., Andorfer, C., Rosenberry, T.L., Lewis, J., Hutton, M., Janus, C., 2007. Accumulation of pathological tau species and memory loss in a conditional model of tauopathy. *J. Neurosci.* 27, 3650–3662. <https://doi.org/10.1523/JNEUROSCI.0587-07.2007>.
- Boland, B., Kumar, A., Lee, S., Platt, F.M., Wegiel, J., Yu, W.H., Nixon, R.A., 2008. Autophagy induction and autophagosome clearance in neurons: relationship to autophagic pathology in Alzheimer's disease. *J. Neurosci.* 28, 6926–6937. <https://doi.org/10.1523/JNEUROSCI.0800-08.2008>.
- Budd, R.C., Yeh, W.-C., Tschopp, J., 2006. cFLIP regulation of lymphocyte activation and development. *Nat. Rev. Immunol.* 6, 196–204. <https://doi.org/10.1038/nri1787>.
- Chen, Q., Kang, J., Fu, C., 2018. The independence of and associations among apoptosis, autophagy, and necrosis. *Signal Transduct. Target. Ther.* 3, 1–11. <https://doi.org/10.1038/s41392-018-0018-5>.
- Deretic, V., Saitoh, T., Akira, S., 2013. Autophagy in infection, inflammation and immunity. *Nat. Rev. Immunol.* 13, 722–737. <https://doi.org/10.1038/nri3532>.
- Dhillon, G., Kaur, S., Pulicharla, R., Brar, S., Cledón, M., Verma, M., Surampalli, R., 2015. Triclosan: current status, occurrence, environmental risks and bioaccumulation potential. *Int. J. Environ. Res. Public Health* 12, 5657–5684. <https://doi.org/10.3390/ijerph120505657>.
- Elmore, S., 2007. Apoptosis: a review of programmed cell death. *Toxicol. Pathol.* 35, 495–516. <https://doi.org/10.1080/01926230701320337>.
- Frank, D., Vaux, D.L., Murphy, J.M., Vince, J.E., Lindqvist, L.M., 2019. Activated MLKL attenuates autophagy following its translocation to intracellular membranes. *J. Cell Sci.* 132, jcs220996. <https://doi.org/10.1242/jcs.220996>.
- Galluzzi, L., Vitale, I., Abrams, J.M., Alnemri, E.S., Baehrecke, E.H., Blagosklonny, M.V., Dawson, T.M., Dawson, V.L., El-Deiry, W.S., Fulda, S., Gottlieb, E., Green, D.R., Hengartner, M.O., Kepp, O., Knight, R.A., Kumar, S., Lipton, S.A., Lu, X., Madeo, F., Malorni, W., Mehlen, P., Nüez, G., Peter, M.E., Piacentini, M., Rubinsztein, D.C., Shi, Y., Simon, H.U., Vandenabeele, P., White, E., Yuan, J., Zhivotovskiy, B., Melino, G., Kroemer, G., 2012. Molecular definitions of cell death subroutines: recommendations of the nomenclature committee on cell death 2012. *Cell Death Differ.* 19, 107–120. <https://doi.org/10.1038/cdd.2011.96>.
- Geens, T., Neels, H., Covaci, A., 2012. Distribution of bisphenol-A, triclosan and n-nonylphenol in human adipose tissue, liver and brain. *Chemosphere* 87, 796–802. <https://doi.org/10.1016/j.chemosphere.2012.01.002>.
- Heras-Sandoval, D., Pérez-Rojas, J.M., Hernández-Damián, J., Pedraza-Chaverri, J., 2014. The role of PI3K/AKT/mTOR pathway in the modulation of autophagy and the clearance of protein aggregates in neurodegeneration. *Cell. Signal.* 26, 2694–2701. <https://doi.org/10.1016/j.cellsig.2014.08.019>.
- Halden, R.U., Lindeman, A.E., Aiello, A.E., Andrews, D., Arnold, W.A., Fair, P., Fuoco, R. E., Greer, L.A., Johnson, P.I., Lohmann, R., McNeill, K., Sacks, V.P., Schettler, T., Weber, R., Zoeller, T.R., Blum, A., 2017. The Florence Statement on Triclosan and Triclocarban. *Environ. Health Perspect.* 125 (6), 1–13. <https://doi.org/10.1289/EHP1788>.
- Jackson, W.T., Giddings jr., T.H., Taylor, M.P., Mulinyawe, S., Rabinovitch, M., Kopito, R.R., Kirkegaard, K., 2005. Subversion of Cellular Autophagosomal Machinery by RNA Viruses. *PLoS Biology* 3 (5), 0861–0871. <https://doi.org/10.1371/journal.pbio.0030156>.
- Jiang, T., Yu, J.T., Zhu, X.C., Tan, M.S., Wang, H.F., Cao, L., Zhang, Q.Q., Shi, J.Q., Gao, L., Qin, H., Zhang, Y.D., Tan, L., 2014. Temsirolimus promotes autophagic clearance of amyloid- $\beta$  and provides protective effects in cellular and animal models of Alzheimer's disease. *Pharmacol. Res.* 81, 54–63. <https://doi.org/10.1016/j.phrs.2014.02.008>.
- Kasibhatla, S., 2006. Acridine Orange/Ethidium Bromide (AO/EB) staining to detect apoptosis. *Cold Spring Harb. Protoc.* 2006, pdb.prot4493-pdb.prot4493. <https://doi.org/10.1101/pdb.prot4493>.
- Kim, J.-Y., Yi, B.-R., Go, R.-E., Hwang, K.-A., Nam, K.-H., Choi, K.-C., 2014. Methoxychlor and triclosan stimulates ovarian cancer growth by regulating cell cycle- and apoptosis-related genes via an estrogen receptor-dependent pathway. *Environ. Toxicol. Pharmacol.* 37, 1264–1274. <https://doi.org/10.1016/j.etap.2014.04.013>.
- Kuboyama, T., Tohda, C., Komatsu, K., 2006. Withanoside IV and its active metabolite, sominone, attenuate  $\beta$ (25–35)-induced neurodegeneration. *Eur. J. Neurosci.* 23, 1417–1426. <https://doi.org/10.1111/j.1460-9568.2006.04664.x>.
- Lee, H.-R., Hwang, K.-A., Nam, K.-H., Kim, H.-C., Choi, K.-C., 2014. Progression of breast cancer cells was enhanced by endocrine-disrupting chemicals, triclosan and octylphenol, via an estrogen receptor-dependent signaling pathway in cellular and mouse xenograft models. *Chem. Res. Toxicol.* 27, 834–842. <https://doi.org/10.1021/tx5000156>.
- Li, F.Y., Jeffrey, P.D., Yu, J.W., Shi, Y., 2006. Crystal structure of a viral FLIP: Insights into FLIP-mediated inhibition of death receptor signaling. *J. Biol. Chem.* 281, 2960–2968. <https://doi.org/10.1074/jbc.M511074200>.
- Liao, C., Kannan, K., 2014. A survey of alkylphenols, bisphenols, and triclosan in personal care products from China and the United States. *Arch. Environ. Contam. Toxicol.* 67, 50–59. <https://doi.org/10.1007/s00244-014-0016-8>.
- Liu, C., Chen, Y., Cui, W., Cao, Y., Zhao, L., Wang, H., Liu, X., Fan, S., Huang, K., Tong, A., Zhou, L., 2021. Inhibition of neuronal necroptosis mediated by RIP1/RIP3/MLKL provides neuroprotective effects on kaolin-induced hydrocephalus in mice. *Cell Prolif.* 54, 1–14. <https://doi.org/10.1111/cpr.13108>.
- Livak, K.J., Schmittgen, T.D., 2001. Analysis of relative gene expression data using real-time quantitative PCR and the 2<sup>-</sup> $\Delta\Delta$ CT method. *Methods* 25, 402–408. <https://doi.org/10.1006/meth.2001.1262>.
- Mandelkow, E.M., Mandelkow, E., 1998. Tau in Alzheimer's disease. *Trends Cell Biol.* 8, 425–427. [https://doi.org/10.1016/S0962-8924\(98\)01368-3](https://doi.org/10.1016/S0962-8924(98)01368-3).
- Mittal, M., Siddiqui, M.R., Tran, K., Reddy, S.P., Malik, A.B., 2014. Reactive oxygen species in inflammation and tissue injury. *Antioxidants Redox Signal.* 20, 1126–1167. <https://doi.org/10.1089/ars.2012.5149>.
- Mosmann, T., 1983. Rapid colorimetric assay for cellular growth and survival: application to proliferation and cytotoxicity assays. *J. Immunol. Methods* 65, 55–63. [https://doi.org/10.1016/0022-1759\(83\)90303-4](https://doi.org/10.1016/0022-1759(83)90303-4).
- Muralidar, S., Ambi, S.V., Sekaran, S., Thirumalai, D., Palaniappan, B., 2020. Role of tau protein in Alzheimer's disease: the prime pathological player. *Int. J. Biol. Macromol.* 163, 1599–1617. <https://doi.org/10.1016/j.ijbiomac.2020.07.327>.
- Murphy, J.M., Czabotar, P.E., Hildebrand, J.M., Lucet, I.S., Zhang, J.G., Alvarez-Diaz, S., Lewis, R., Lalaoui, N., Metcalf, D., Webb, A.I., Young, S.N., Varghese, L.N., Tannahill, G.M., Hatchell, E.C., Majewski, I.J., Okamoto, T., Dobson, R.C.J., Hilton, D.J., Babon, J.J., Nicola, N.A., Strasser, A., Silke, J., Alexander, W.S., 2013. The pseudokinase MLKL mediates necroptosis via a molecular switch mechanism. *Immunity* 39, 443–453. <https://doi.org/10.1016/j.immuni.2013.06.018>.
- Muth-Köhne, E., Wichmann, A., Delov, V., Fenske, M., 2012. The classification of motor neuron defects in the zebrafish embryo toxicity test (ZFET) as an animal alternative approach to assess developmental neurotoxicity. *Neurotoxicol. Teratol.* 34, 413–424. <https://doi.org/10.1016/j.ntt.2012.04.006>.
- Nixon, R.A., 2013. The role of autophagy in neurodegenerative disease. *Nat. Med.* 19, 983–997. <https://doi.org/10.1038/nm.3232>.
- Park, B.K., Gonzales, E.L.T., Yang, S.M., Bang, M., Choi, C.S., Shin, C.Y., 2016. Effects of triclosan on neural stem cell viability and survival. *Biomol. Ther.* 24, 99–107. <https://doi.org/10.4062/biomolther.2015.164>.
- Pasparakis, M., Vandenabeele, P., 2015. Necroptosis and its role in inflammation. *Nature* 517, 311–320. <https://doi.org/10.1038/nature14191>.
- Paul, K.B., Hedge, J.M., DeVito, M.J., Crofton, K.M., 2010. Short-term exposure to triclosan decreases thyroxine in vivo via upregulation of hepatic catabolism in young Long-Evans rats. *Toxicol. Sci.* 113, 367–379. <https://doi.org/10.1093/toxsci/kfp271>.
- Pierzyńska-Mach, A., Janowski, P.A., Dobrucki, J.W., 2014. Evaluation of acridine orange, LysoTracker Red, and quinacrine as fluorescent probes for long-term tracking of acidic vesicles. *Cytom. Part A* 85, 729–737. <https://doi.org/10.1002/cyto.a.22495>.
- Raut, S.A., Angus, R.A., 2010. Triclosan has endocrine-disrupting effects in male western mosquitofish, *Gambusia affinis*. *Environ. Toxicol. Chem.* 29, 1287–1291. <https://doi.org/10.1002/etc.150>.
- Runwal, G., Stamatakou, E., Siddiqi, F.H., Puri, C., Zhu, Y., Rubinsztein, D.C., 2019. LC3-positive structures are prominent in autophagy-deficient cells. *Sci. Rep.* 9, 10147. <https://doi.org/10.1038/s41598-019-46657-z>.
- Szychowski, K.A., Rybczyńska-Tkaczyk, K., Gmiński, J., Wójtowicz, A.K., 2020. The interference of alpha- and beta-naphthoflavone with triclosan effects on viability, apoptosis and reactive oxygen species production in mouse neocortical neurons. *Pestic. Biochem. Physiol.* 168, 1–13. <https://doi.org/10.1016/j.pestbp.2020.104638>.
- Szychowski, K.A., Sitarz, A.M., Wojtowicz, A.K., 2015. Triclosan induces Fas receptor-dependent apoptosis in mouse neocortical neurons in vitro. *Neuroscience* 284, 192–201. <https://doi.org/10.1016/j.neuroscience.2014.10.001>.
- Tabari, S.A., Esfahani, M.L., Hosseini, S.M., Rahimi, A., 2019. Neurobehavioral toxicity of triclosan in mice. *Food Chem. Toxicol.* 130, 154–160. <https://doi.org/10.1016/j.fct.2019.05.025>.
- Tait, S.W.G., Green, D.R., 2008. Caspase-independent cell death: leaving the set without the final cut. *Oncogene* 27, 6452–6461. <https://doi.org/10.1038/onc.2008.311>.
- Tsapras, P., Nezis, I.P., 2017. Caspase involvement in autophagy. *Cell Death Differ.* 24, 1369–1379. <https://doi.org/10.1038/cdd.2017.43>.
- Van Der Meer, T.P., Artacho-Córdón, F., Swaab, D.F., Struik, D., Makris, K.C., Wolfenbutter, B.H.R., Frederiksen, H., Van Vliet-Ostapchouk, J.V., 2017. Distribution of non-persistent endocrine disruptors in two different regions of the human brain. *Int. J. Environ. Res. Public Health* 14, 1059. <https://doi.org/10.3390/ijerph14091059>.
- Varshney, R., Gupta, S., Roy, P., 2017. Cytoprotective effect of kaempferol against palmitic acid-induced pancreatic  $\beta$ -cell death through modulation of autophagy via AMPK/mTOR signaling pathway. *Mol. Cell. Endocrinol.* 448, 1–20. <https://doi.org/10.1016/j.mce.2017.02.033>.
- Vogel, J.W., Young, A.L., Oxtoby, N.P., Smith, R., Ossenkoppe, R., Strandberg, O.T., Joie, R. La, Aksman, L.M., Grothe, M.J., Devous, M.D., Rabinovici, G.D., Alexander,

- D.C., Lyoo, C.H., Evans, A.C., Hansson, O., Alzheimer's Disease Neuroimaging Initiative. 2021. Four distinct trajectories of tau deposition identified in Alzheimer's disease. *Nat. Med.* 27(5), 871-881. <https://doi.org/10.1038/s41591-021-01309-6>.
- Wander, C.M., Tseng, J.-H., Song, S., Al Housseiny, H.A., Tart, D.S., Ajit, A., Ian Shih, Y.-Y., Lobrovich, R., Song, J., Meeker, R.B., Irwin, D.J., Cohen, T.J., 2020. The accumulation of tau-immunoreactive hippocampal granules and corpora amylacea implicates reactive glia in tau pathogenesis during aging. *iScience* 23 (7), 101255.
- Wang, D.D., Jin, M.F., Zhao, D.J., Ni, H., 2019. Reduction of mitophagy-related oxidative stress and preservation of mitochondria function using melatonin therapy in an HT22 hippocampal neuronal cell model of glutamate-induced excitotoxicity. *Front. Endocrinol. (Lausanne)* 10, 1–14. <https://doi.org/10.3389/fendo.2019.00550>.
- Wang, X., Chen, X., Feng, X., Chang, F., Chen, M., Xia, Y., Chen, L., 2015. Triclosan causes spontaneous abortion accompanied by decline of estrogen sulfotransferase activity in humans and mice. *Sci. Rep.* 5, 18252. <https://doi.org/10.1038/srep18252>.
- Wilburn, W.J., Jamal, S., Ismail, F., Brooks, D., Whalen, M., 2021. Evaluation of triclosan exposures on secretion of pro-inflammatory cytokines from human immune cells. *Environ. Toxicol. Pharmacol.* 83,. <https://doi.org/10.1016/j.etap.2021.103599> 103599.
- Yuan, J., Yankner, B.A., 2000. Apoptosis in the nervous system. *Nature* 407, 802–809. <https://doi.org/10.1038/35037739>.
- Zheng, X., Yan, Z., Liu, P., Fan, J., Wang, S., Wang, P., Zhang, T., 2019. Research progress on toxic effects and water quality criteria of triclosan. *Bull. Environ. Contam. Toxicol.* 102, 731–740. <https://doi.org/10.1007/s00128-019-02603-3>.